^{67}Zn Mössbauer investigation of Cu-Zn alloys at high pressure

W. Adlassnig, W. Potzel, J. Moser, W. Schiessl, U. Potzel, C. Schäfer,
M. Steiner, H. Karzel, M. Peter, and G. M. Kalvius
Physik-Department (E15), Technische Universität München, D-8046 Garching bei München, Federal Republic of Germany
(Received 25 April 1989)

The narrow 93.3-keV Mössbauer resonance in ^{67}Zn was used to investigate Cu-Zn alloys (brass) containing 16.6 wt. % Zn (α phase), 50.5 wt. % Zn (β' phase), and 44.1 wt. % Zn (α-β' mixed phase) under pressures up to 6.2 GPa and at 4.2 K. In the three systems the recoil-free fraction and the center shift change linearly with reduced volume. The decrease of the center shift is due to the second-order Doppler effect, which is partially compensated by the increase of the *s*-electron density at the ^{67}Zn nucleus when the conduction electrons are compressed. In α-brass, short-range order leads to four different Cu-Zn configurations, one of which exhibits a center shift which nearly coincides with that of the β' phase. At 4.2 K and under high pressures, β'-brass is partially transformed into a new phase which might be caused by a low-temperature martensitic transition. However, no phase transformation from the β' to the α phase is observed.

I. INTRODUCTION

Cu-Zn alloys (brass) are of great technological interest and have provoked a large number of theoretical investigations[1–7] to calculate electronic properties of the various crystallographic phases. The phase diagram[8] is depicted in Fig. 1. The brass system is the prime representative of the so-called Hume-Rothery alloys, named after Hume-Rothery, who already in the 1920's formulated his famous rules.[9] They emphasized the importance of the average concentration of conduction electrons in determining structural phase transitions. Unfortunately, up to now, modern theoretical calculations (e.g., Refs. 1 and 2) have not been able to corroborate the Hume-Rothery rules. We have tried to investigate this question experimentally by using the 93.3-keV Mössbauer transition in ^{67}Zn. Due to its extremely narrow width, this Mössbauer resonance is well suited for determining small changes of hyperfine interactions, in particular of isomer shifts. In addition, this resonance is also a highly sensitive tool for investigating lattice-dynamical effects, the anisotropy of the recoil-free fraction, and the second-order Doppler shift.[10–12] Thus complementary information concerning the strength and anisotropy of the chemical bond can be obtained. Furthermore, we want to emphasize that Zn itself is one alloying partner. Therefore we do not have to introduce into the alloying system a Mössbauer isotope as an impurity, which often significantly changes the electronic structure as compared to the pure alloy.[13]

We have proceeded on two routes. Firstly, we studied all major phases of the brass system. The main results have already been published:[14–16] Most startling is the observation of short-range order in the α phase[14,15] in contrast to the expected binomial distribution of Zn in Cu. In the α phase the preferred Cu-Zn configurations can quantitatively be described within the Cu_3Zn structure by an appropriate order parameter.[15] The β' phase exhibits a single narrow absorption line, indicating that the ordered CsCl structure is present. Surprisingly, the *s*-electron density at the ^{67}Zn nucleus in the β' phase is lower than that in the α phase. In the γ phase, two inequivalent Zn sites were found with highly different chemical bondings and electronic structures.[14]

Secondly, we have searched for crystallographic phase transitions which might occur when external pressure is applied. In particular we were interested in transitions between the α and β' phases with fcc and bcc structures, respectively. Such transitions might be caused by changes of the conduction-electron density. We built a special high-resolution high-pressure Mössbauer spectrometer for the 93.3-keV resonance in ^{67}Zn.[17] It was used to investigate alloys of α-brass containing 16.6 wt. % Zn, of β'-brass with 50.5 wt. % Zn, and of a (α,β') mixed phase with 44.1 wt. % Zn under pressures up to 6.2 GPa at 4.2 K. In addition, the compressibilities of

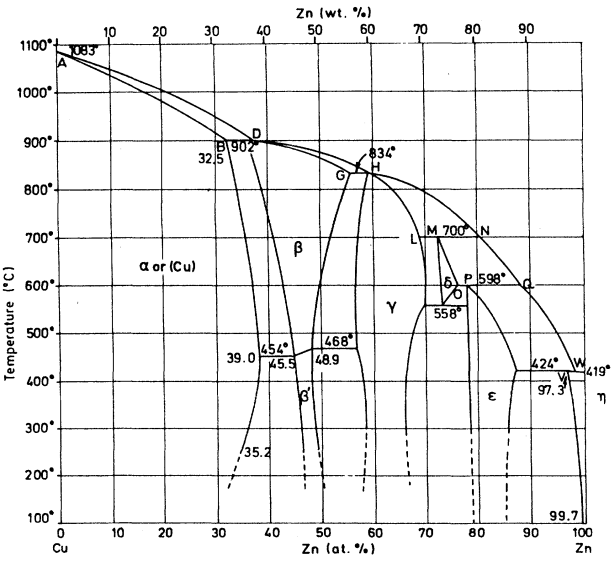

FIG. 1. Phase diagram of the Cu-Zn system.

these alloys were determined by high-pressure x-ray diffraction using a Guinier-type spectrometer.[18] The results of the high-pressure experiments are described in the present paper.

II. EXPERIMENTAL DETAILS

A. Doppler-velocity spectrometer for high pressures

A high-pressure, low-temperature Mössbauer spectrometer for the 93.3-keV resonance in ^{67}Zn was developed. The design has been described elsewhere.[17,12] Only the basic features will be mentioned here. As shown in Fig. 2, the main components of the high-pressure spectrometer are the piezoelectric drive and the pressure clamp. The Doppler drive, which acts on the source, is mounted directly on top of the pressure clamp to avoid unwanted vibrational motions between source and absorber, which could cause distortions of the absorption lines.

The pressure is applied to the absorber by two symmetrical anvils made of B_4C. The absorber is embedded in talcum powder, which serves as a pressure-transmitting medium and ensures quasihydrostatic conditions. The small Lamb-Mössbauer factors (typically 1%) demand the use of absorbers with large dimensions ($\sim$7 mm in diameter, $\sim$2 mm in height) if Mössbauer spectra with good statistical accuracy are to be obtained. The large height of the sample requires the application of a sandwich gasket[17,19] consisting of four tantalum and five pyrophyllite rings. The gasket acts in addition as a collimator for the 93.3-keV γ radiation. The whole system is inserted from the top into the liquid-He vessel of a conventional metal cryostat. The pressure at the absorber is measured *in situ* by a lead manometer,[17] which uses the known pressure dependence of the superconducting transition temperature of lead as a gauge.[20] Quasihydrostatic pressures up to 6.2 GPa with gradients smaller than 10% were obtained.

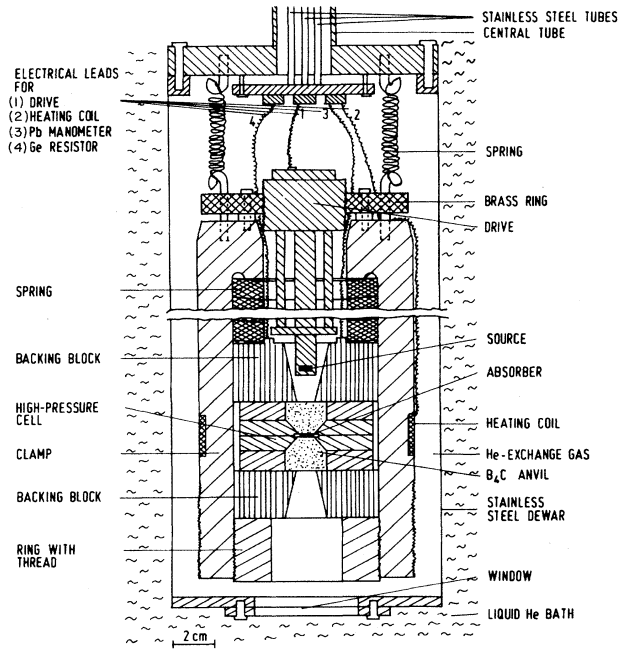

FIG. 2. High-pressure clamp with piezoelectric quartz drive as mounted inside the He cryostat.

In order to decouple the spectrometer from mechanical vibrations of the boiling helium and of the cryostat, the whole system is suspended by springs inside a sealed stainless-steel dewar (see Fig. 2) filled with He-exchange gas. To change pressure, the clamp together with the piezo drive have to be warmed up to room temperature.

B. Source and absorber preparation

As a Mössbauer source we used ^{67}Ga in Cu, which exhibits a single emission line.[21] The ^{67}Ga($T_{1/2}=78$ h) activity was produced *in situ* by 46-MeV α bombardment of Cu disks with natural abundance of the Cu isotopes. The disks were 8 mm in diameter and 0.5 mm in thickness. The sources were used without annealing about 24 h after the end of irradiation.

The brass alloys were melted from high-purity copper (99.99% purity) and from zinc metal enriched to $\sim$91% in ^{67}Zn. At temperature T_M (above the melting point of the alloy) both metals reacted in a high-purity (reactor grade) graphite crucible sealed within a quartz ampulla filled with argon. Thereafter the alloy was annealed at temperature T_A for several hours (Δt) inside the quartz ampulla and slowly (50 K/h) cooled to room temperature. Temperatures T_M and T_A as well as annealing times are summarized in Table I. The values for the absorber thickness (n) are also given. The copper concentrations of the alloys were determined electrolytically.[22] Part of each alloy was used for compressibility measurements using an x-ray diffractometer of the Guinier type.[18]

C. Velocity calibration and nuclear pulse counting

Doppler velocities were calibrated using the known quadrupole interactions in ^{67}Zn metal,[23,24] which was measured previously by the frequency-modulation technique.[25] The nuclear-pulse-counting chain consisted of an intrinsic Ge detector of 10 mm thickness and 40 mm diameter coupled to fast amplifiers and a fast single-channel analyzer.[26] Typical signal-to-background ratios of $S/(S+B)\sim0.75$ were obtained at count rates up to 100 000 s^{-1} in the 93.3-keV window. The data pulses were collected in time mode into a 512-channel analyzer

TABLE I. Details of absorber preparation. c_{Zn} is the concentration of zinc, T_M the temperature at which the metals were melted to form the alloy. T_A and Δt specify temperature and time of the annealing process, respectively. The absorber thickness n is also given.

c_{Zn} (wt. %)	n (g/cm^2 ^{67}Zn)	T_M (K)	T_A (K)	Δt (h)
16.6	0.255	1388	1073	38
44.1	0.595	1273	723	68
50.5	0.650	1273	653	127

whose channel advance rate was synchronized to the drive frequency by a phase-locked-loop circuit.[27] To obtain Mössbauer spectra with good statistical accuracy, measuring times of up to three weeks were necessary.

III. RESULTS

A. α-brass containing 16.6 wt. % Zn

Figure 3 displays Mössbauer absorption spectra recorded at 4.2 K and four different pressures. The spectra could well be fitted by a superposition of only four independent Lorentzian lines. The results are summarized in Table II. The pressure dependence of the Lamb-Mössbauer factor (LMF) as derived from the total area under the absorption lines is given in Table III. The following results are particularly remarkable.

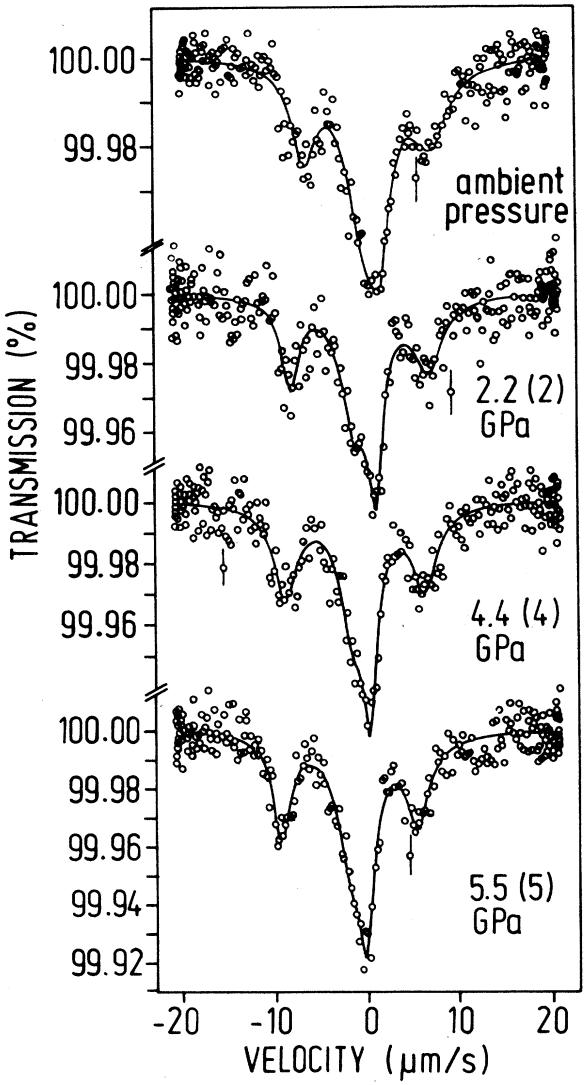

FIG. 3. Mössbauer absorption spectra of α-brass with 16.6 wt. % Zn recorded at 4.2 K and four different pressures. The source is ^{67}Ga in Cu also at 4.2 K.

(i) The LMF increases with pressure.

(ii) All four line positions decrease when pressure is applied. Lines L_2, L_3, and L_4 shift by about equal amounts, whereas L_1 moves faster by a factor of ~ 1.5.

(iii) The relative absorption areas under the four lines are independent of pressure within the experimental accuracy.

(iv) All changes of the Mössbauer parameters are reversible, i.e., after releasing the pressure, the original values are resumed within the experimental error limits.

B. Mixed phase (α,β') containing 44.1 wt. % Zn

Figure 4 shows Mössbauer absorption spectra obtained at 4.2 K and two different pressures. Also in this case the spectra were fitted by a superposition of four independent Lorentzian lines. Table IV gives the results, which can be summarized as follows.

(i) The LMF increases with pressure.

(ii) All four lines move to more negative positions when pressure is applied. Again, the line with the most negative position changes faster than the others.

(iii) Within experimental accuracy the relative absorption areas do not change with pressure; in particular, there is no transformation from β' to α phase or vice versa.

(iv) All changes of the Mössbauer parameters are reversible.

C. β'-brass containing 50.5 wt. % Zn

Figure 5 displays Mössbauer absorption spectra taken at 4.2 K and five different pressures. The spectrum at ambient pressure exhibits a single Lorentzian, whereas at

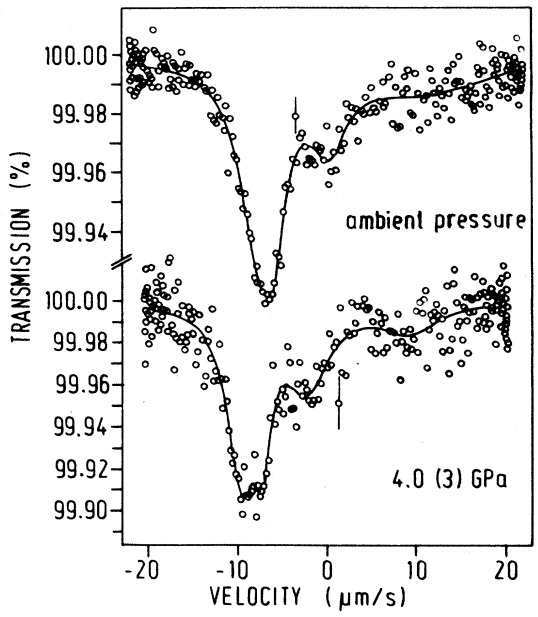

FIG. 4. Mössbauer absorption spectra of brass in the (α,β') mixed phase with 44.1 wt. % Zn recorded at 4.2 K and two different pressures. The source is ^{67}Ga in Cu also at 4.2 K.

TABLE II. Summary of measured Mössbauer parameters for α-brass (16.6 wt. % Zn) at 4.2 K and various pressures. Only statistical errors are quoted for position, width, and area. The last four lines give the results after releasing the pressure to demonstrate reversibility of the Mössbauer parameters.

Pressure (GPa)	Position (μm/s)	Width (μm/s)	Area (% μm/s)
ambient pressure	−6.48±0.15	3.05±0.52	0.061±0.010
	0.00±0.10	4.54±0.58	0.160±0.021
	1.73±0.16	2.48±0.54	0.066±0.017
	7.20±0.25	4.71±0.84	0.078±0.014
2.2±0.2	−8.13±0.15	2.32±0.47	0.060±0.010
	−1.20±0.34	3.51±0.83	0.121±0.038
	1.06±0.12	1.96±0.43	0.093±0.029
	6.85±0.25	4.03±0.84	0.083±0.014
4.4±0.4	−8.90±0.15	3.11±0.51	0.090±0.012
	−1.63±0.47	3.50±0.89	0.126±0.056
	0.24±0.12	2.01±0.45	0.114±0.045
	6.27±0.17	3.36±0.57	0.090±0.013
5.5±0.5	−9.41±0.10	2.27±0.32	0.079±0.009
	−1.88±0.58	3.72±0.81	0.147±0.073
	−0.23±0.14	1.99±0.55	0.107±0.060
	5.37±0.15	3.24±0.50	0.096±0.013
ambient pressure	−6.82±0.39	3.32±1.35	0.045±0.018
	0.00±0.10	5.66±3.60	0.074±0.052
	1.51±0.41	3.25±1.04	0.092±0.045
	7.58±0.23	1.99±0.76	0.032±0.010

higher pressures two absorption lines are observed which are only partially resolved. Table V summarizes the results obtained from fits of independent Lorentzian lines. Most remarkable are the following observations.

(i) The LMF increases by almost a factor of 2 when the external pressure reaches 6.2 GPa.

(ii) Already at ~1 GPa two absorption lines are observed. At higher pressures the two lines move to more negative velocities with slightly different rates.

(iii) Within experimental accuracy the relative intensities of the two lines are independent of pressure above ~1 GPa.

(iv) All changes of the Mössbauer parameters are reversible.

D. Compressibility measurements

X-ray-diffraction measurements were performed at room temperature up to ~10 GPa on a Guinier-type spectrometer.[18] The pressure dependence of the lattice constants was fitted by the Birch-Murnaghan equation.[28] Figure 6 shows the pressure dependence of the volume of the three alloys investigated. Table VI gives the results for the lattice constants, the bulk moduli B_0, and for B_0', which represents a measure for the change of B_0 with pressure. Neither phase transitions nor hysteresis effects are detectable in the whole pressure range. The bulk moduli of the mixed (α,β') absorber tend to be lower than in the pure phases.

TABLE III. Change of Lamb-Mössbauer factor (LMF) with pressure for brass alloys with three different concentrations (c_{Zn} = 16.6, 44.1, and 50.5 wt. %).

c_{Zn} = 16.6 wt. %		c_{Zn} = 44.1 wt. %		c_{Zn} = 50.5 wt. %	
Pressure (GPa)	LMF (%)	Pressure (GPa)	LMF (%)	Pressure (GPa)	LMF (%)
ambient pressure	1.99±0.11	ambient pressure	1.51±0.44	ambient pressure	1.29±0.06
2.2±0.2	2.83±0.15	4.0±0.3	2.06±0.31	1.1±0.1	1.33±0.06
4.4±0.4	3.24±0.17	5.8±0.4	1.90±0.35	3.2±0.3	1.64±0.06
5.5±0.5	3.37±0.18			4.4±0.3	1.85±0.08
				6.2±0.3	2.27±0.08

TABLE IV. Summary of measured Mössbauer parameters for brass in the (α,β') mixed phase with 44.1 wt. % Zn at 4.2 K and various pressures. Only statistical errors are quoted for position, width, and area. The last four lines give the results after releasing the pressure to demonstrate reversibility of the Mössbauer parameters.

Pressure (GPa)	Position (μm/s)	Width (μm/s)	Area (% μm/s)
ambient pressure	−6.95±0.65	4.51±0.61	0.245±0.132
	−5.31±0.34	2.76±1.14	0.106±0.115
	0.31±0.23	4.43±1.03	0.105±0.029
	9.93±1.40	17.19±4.94	0.204±0.074
4.0±0.3	−9.59±0.25	3.74±0.57	0.292±0.064
	−7.23±0.18	2.15±0.74	0.115±0.055
	−2.15±0.36	5.79±1.36	0.219±0.049
	9.24±0.93	7.86±3.36	0.108±0.046
5.8±0.4	−10.80±0.25	3.38±0.69	0.194±0.062
	−7.90±0.25	3.57±0.88	0.224±0.074
	−2.21±0.31	4.01±1.18	0.122±0.035
ambient pressure	−8.32±0.19	2.14±0.65	0.049±0.017
	−5.50±0.13	2.83±0.51	0.125±0.024
	0.77±0.48	6.25±1.94	0.098±0.030
	12.06±1.68	8.94±5.64	0.041±0.026

IV. DISCUSSION

A. Lamb-Mössbauer factor

The volume dependences of the Lamb-Mössbauer factor f for the α (16.6 wt. % Zn) and β' (50.5 wt. % Zn) phases are depicted in Fig. 7. We have assumed that within each phase the different configurations (four in α- and two in β'-brass) have the same f factor. Thus f^{α} and $f^{\beta'}$ are directly proportional to the total area under the absorption lines of the α and β' absorber, respectively. In both cases a linear relation is found. The straight-line fits give the results

$$f^{\alpha}=[(2.05\pm0.10)+(46.3\pm6.2)(1-V/V_0)]\% ,$$

$$f^{\beta'}=[(1.223\pm0.045)+(25.8\pm2.6)(1-V/V_0)]\% .$$

The increase in f is surprisingly large. Within the Debye model it can be expressed by an increase of the effective Debye temperature Θ_{eff}. From our data we deduce $\Theta^{\alpha}_{\text{eff}}=309\pm4$ K at 4.2 K and ambient pressure and $\Theta^{\alpha}_{\text{eff}}=357\pm5$ K at 4.2 K and 5.5 GPa. The corresponding values for the β' phase are $\Theta^{\beta'}_{\text{eff}}=278\pm3$ K (ambient pressure) and $\Theta^{\beta'}_{\text{eff}}=320\pm3$ K at 6.2 GPa. Together with our data on the bulk moduli the increase of Θ would result in Grüneisen parameters $\gamma^{\alpha}\simeq4.9$ and $\gamma^{\beta'}\simeq4.0$. Both values

TABLE V. Summary of measured Mössbauer parameters for β'-brass (50.5 wt. % Zn) at 4.2 K and various pressures. Only statistical errors are quoted for position, width, and area. The last line gives the results after releasing the pressure to demonstrate reversibility of the Mössbauer parameters.

Pressure (Gpa)	Position (μm/s)	Width (μm/s)	Area (% μm/s)
ambient pressure	−6.11±0.03	2.28±0.10	0.501±0.016
1.1±0.1	−8.19±0.09	1.19±0.34	0.078±0.031
	−6.75±0.09	2.25±0.20	0.323±0.039
3.2±0.3	−9.15±0.06	0.90±0.29	0.061±0.026
	−7.83±0.09	2.63±0.16	0.452±0.038
4.4±0.3	−10.03±0.14	1.86±0.40	0.149±0.048
	−8.30±0.09	2.30±0.23	0.393±0.054
6.2±0.3	−11.16±0.09	1.31±0.34	0.094±0.029
	−9.18±0.06	2.81±0.17	0.617±0.041
ambient pressure	−6.05±0.04	1.81±0.10	0.302±0.013

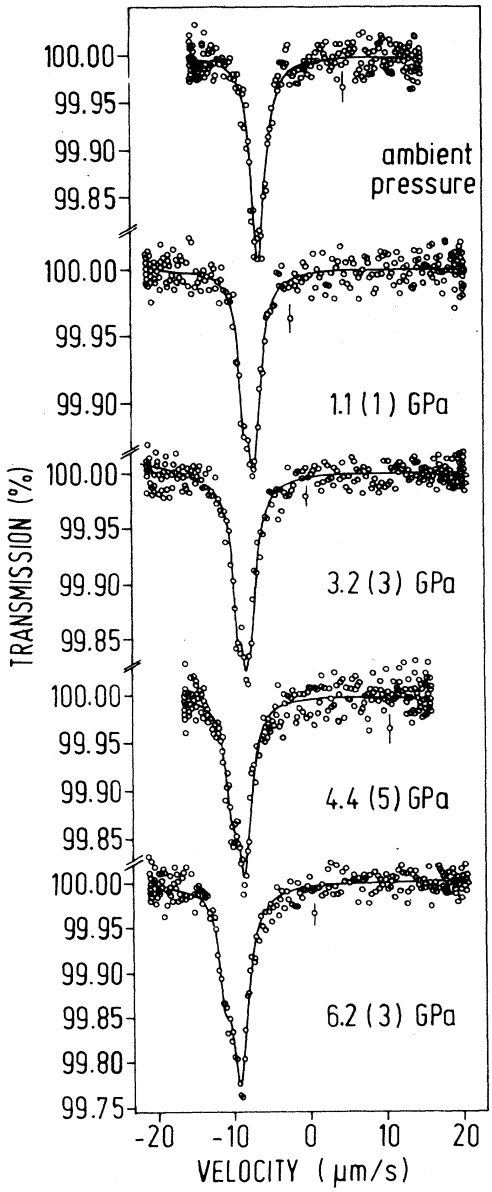

FIG. 5. Mössbauer absorption spectra of β'-brass with 50.5 wt. % Zn recorded at 4.2 K and five different pressures. The source is ^{67}Ga in Cu also at 4.2 K.

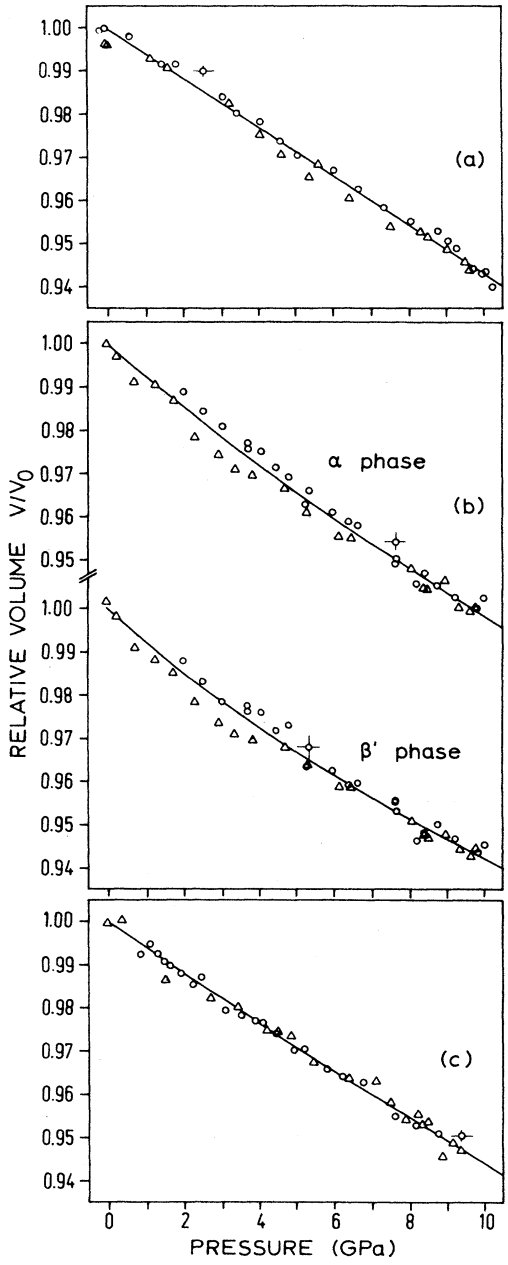

FIG. 6. Pressure dependence of the volume of the unit cell for brass alloys with Zn concentrations of (a) 16.6 wt. %, (b) 44.1 wt. %, and (c) 50.5 wt. %. X-ray data were taken at room temperature.

TABLE VI. Summary of the compressibility measurements on brass alloys with three different concentrations (c_{Zn}). The values given for the lattice constant (a), the bulk modulus (B_0), and its pressure dependence (B_0') are results of fits by the Birch-Murnaghan equation. The alloy with $c_{Zn}=44.1$ wt. % is a mixed (α,β') phase.

c_{Zn} (wt. %)	a (Å)	B_0 (GPa)	B_0'
16.6	3.652±0.002	171.8±2.7	0
44.1	3.692±0.002	134.6±14.6	4.3±2.8
44.1	2.940±0.002	125.4±18.2	10.0±4.5
50.5	2.946±0.001	163.4±10.7	1.9±2.0

appear too large by a factor of ~2. This discrepancy is not understood at present. Although the Debye approximation usually represents only a crude model for lattice-dynamical effects at elevated temperatures, it is expected to be acceptable in the low-temperature limit (4.2 K) for cubic systems. In addition, the masses of the two alloying partners differ only by about 5%. If such large Grüneisen parameters would be valid, the bonding between Cu and Zn atoms in the alloy should strongly in-

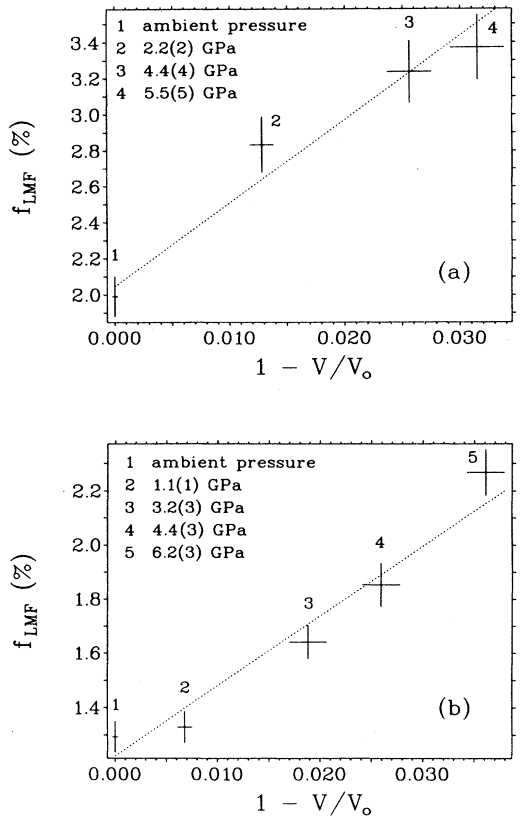

FIG. 7. Volume dependence of the Lamb-Mössbauer factor for brass alloys with Zn concentrations of (a) 16.6 wt. % and (b) 50.5 wt. %. The straight lines are least-squares fits to the data points.

crease and give rise to the observed changes in f. A similar situation has recently been found for Zn metal under high external pressure.[12] Modern cluster calculations which can give reliable values for force constants between atoms will be able to clarify this discrepancy. Unfortunately, they are not available at present.

B. Center shift

1. α-brass

The Mössbauer spectrum of the α-brass (16.6 wt. % Zn) at 4.2 K and ambient pressure (see Fig. 3) shows four absorption lines. Additional measurements on absorbers with Zn concentrations of 4.5, 10.5, and 25.9 wt. % gave similar spectra:[14,15] within the α phase, changing Zn concentration affects the relative intensities of the four peaks but not their positions. This has been interpreted by the presence of short-range order which gives rise to only four different Cu-Zn configurations in α-brass[14,15] instead of the expected binomial distribution. The absorption line at 0 μm/s (unshifted with respect to the emission line of the source) is to be identified with a configuration of one Zn atom surrounded by 12 nearest Cu neighbors, i.e., the same Cu-Zn configuration as in the source. The absorption lines at positive velocities are caused by Cu-Zn configurations where the s-electron density at the Zn nucleus is increased. In these configurations the nearest-neighbor shell (12 atoms) contains several Zn atoms. The relative intensities of the absorption lines do not fit a binomial distribution but can well be described within the Cu_3Zn structure by an appropriate order parameter.[15]

When pressure is applied, the relative intensities of the four absorption lines do not change, i.e., the short-range order is not affected when the volume of the unit cell is reduced. The line positions, however, change markedly. This is demonstrated by Fig. 8. The straight-line fits give the results (in units of μm/s)

$$S_{L_1} = -(6.62 \pm 0.14) - (93.1 \pm 7.6)(1 - V/V_0)\ \mu\text{m/s}\ ,$$

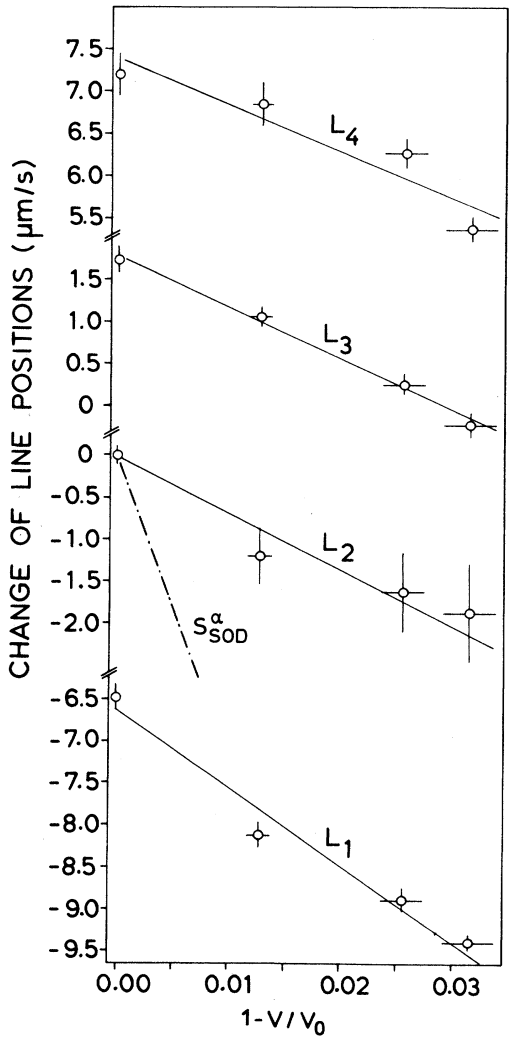

FIG. 8. Change of line positions of α-brass (16.6 wt. % Zn) with reduced volume of the unit cell. The straight lines are least-squares fits to the data points. Absorption line L_1 changes faster than the other three. The expected change due to the second-order Doppler shift S_{SOD} is also indicated.

$$S_{L_2} = -(0.02 \pm 0.10) - (67.4 \pm 12.8)(1 - V/V_0)\ \mu\text{m/s} ,$$

$$S_{L_3} = (1.78 \pm 0.13) - (61.3 \pm 7.1)(1 - V/V_0)\ \mu\text{m/s} ,$$

$$S_{L_4} = (7.38 \pm 0.22) - (55.3 \pm 9.5)(1 - V/V_0)\ \mu\text{m/s} .$$

Whereas lines L_2, L_3, and L_4 exhibit the same slope of $dS/d(1-V/V_0) \sim -60\ \mu$m/s within the error limits, L_1 gives a much steeper slope. In fact, within our experimental accuracy, $dS_{L_1}/d(1-V/V_0)$ agrees with the results found for β'-brass (see below). However, not only the slope but also the center shift at ambient pressure is very close to that of β'-brass. These coincidences are very surprising, since the crystallographic structures of α- and β'-brass are quite different.

The line shifts result from two counteracting effects.

(i) The second-order Doppler effect causes a shift S_{SOD} to more negative velocities because of the increase of the effective Debye temperature.

(ii) The increase of the electron density $\rho(0)$ at the Zn nucleus with reduced volume leads to a shift to more positive velocities.

The SOD can be estimated within the Debye model, which is expected to be reliable (see discussion of LMF). Using the values for Θ_{eff} derived from the Lamb-Mössbauer factors we get (in units of μm/s)

$$S^{\alpha}_{\text{SOD}} = -(0.6 \pm 0.9) - (364 \pm 47)(1 - V/V_0)\ \mu\text{m/s} ,$$

which is also given in Fig. 8. Similar to the case of the LMF we have assumed that the SOD is the same for the four Cu-Zn configurations. The difference $(S_{L_i} - S^{\alpha}_{\text{SOD}})$ corresponds to the increase of the electron density $\rho_i(0)$ at the Zn nucleus which belongs to the Cu-Zn configuration represented by L_i. The increase of $\rho_i(0)$ is surprisingly large for all Cu-Zn configurations: it is, for example, a factor of ~ 3 bigger than for Zn metal.[12] The increase of $\rho_i(0)$ is about equal for the Cu-Zn configurations giving rise to the absorption lines L_2, L_3, and L_4, but is smaller by a factor of ~ 1.12 for L_1.

Most puzzling is the line L_1 at negative Doppler velocities. In a simple band-structure model, the number of conduction electrons, and thus the s-electron density $\rho(0)$ at the Zn nucleus, increases with Zn concentration. For this reason the absorption lines of all four Cu-Zn configurations in α-brass are expected to exhibit zero or positive Doppler velocities with respect to the source (highly diluted ^{67}Zn in Cu). Our data show that not only the position of L_1 but also its change with reduced volume coincides with the corresponding values of β'-brass. Therefore, on the basis of the Mössbauer results it might be tempting to identify L_1 with the β' phase. This, however, would contradict the generally accepted phase diagram (see Fig. 1). Also, our room-temperature x-ray data show no indications of a β'-type phase. The coincidences mentioned above might therefore be only fortuitous, although a hypothetical Cu-Zn phase diagram published recently[29] indicates that at low temperatures the region of the β' phase extends to very low Zn concentrations and does not allow the exclusion of a partial formation of β-brass.

From still another point of view, one might argue that the four Cu-Zn configurations, although belonging to the same crystallographic phase, should have different Lamb-Mössbauer factors and second-order Doppler shifts. In particular, the negative ($-6.62\ \mu$m/s) S_{L_1} might be caused just by the second-order Doppler shift alone. This would require a difference in Debye temperature of ~ 29 K. As a consequence, the LMF at ambient pressure would be $\sim 40\%$ larger for L_1 than for the other lines. Although such a difference in LMF appears quite large within the same crystallographic structure, this possibility cannot be ruled out. Again, modern theoretical calculations are called for to bring more insight into these questions.

2. β'-brass

Below ~ 725 K, β'-brass forms an ordered alloy with CsCl structure, i.e., each Zn atom is surrounded by eight Cu atoms. As expected for a cubic structure, the Mössbauer spectrum obtained at 4.2 K and ambient pressure exhibits a single (rather narrow) Lorentzian line. Its position is shifted to negative velocities ($\sim -6.1\ \mu$m/s) with respect to the source ^{67}Zn in fcc Cu, where each ^{67}Zn atom is surrounded by 12 Cu atoms in the nearest-neighbor shell. This shift cannot be caused by the second-order Doppler effect, since the effective Debye temperature of the source is higher than that for β'-brass. As a consequence, $\rho(0)$ has to be lower in β'-brass than at the highly diluted Zn sites in fcc Cu. This has been attributed to an increased shielding effect of the rather narrow $3d$ band of Zn in β'-brass as compared to α-brass.[30,16,14]

Most surprisingly, the single absorption line of β'-brass splits into a doublet when pressure is applied. The change of line positions is depicted in Fig. 9. The straight-line fits give the results (in μm/s)

$$S_{D_1} = -(7.47 \pm 0.15) - (99.6 \pm 7.5)(1 - V/V_0)\ \mu\text{m/s} ,$$

$$S_{D_2} = -(6.12 \pm 0.03) - (86.0 \pm 3.7)(1 - V/V_0)\ \mu\text{m/s} .$$

The slopes are slightly different, just barely outside our experimental accuracy. Both values are close to the result found for line L_1 in α-brass.

Using the values for Θ_{eff} derived from the Lamb-Mössbauer factors, we get for the second-order Doppler shift (in units of μm/s)

$$S^{\beta'}_{\text{SOD}} = (0.74 \pm 0.54) - (268 \pm 27)(1 - V/V_0)\ \mu\text{m/s} .$$

The difference $(S_{D_i} - S^{\beta'}_{\text{SOD}})$ gives the increase of $\rho(0)$. This increase is a factor of ~ 1.5 smaller than for the α-phase absorber. This result[31] is surprising because, as al-

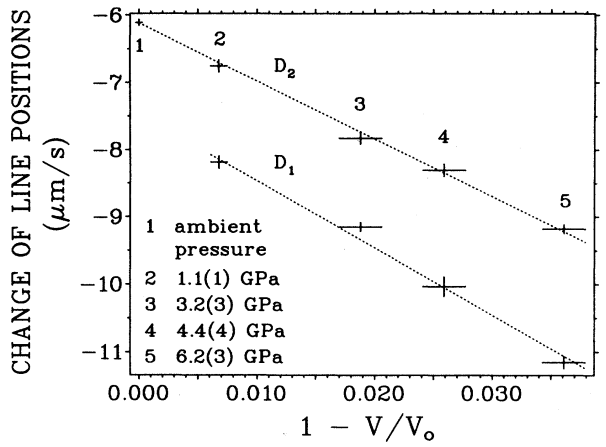

FIG. 9. Change of line positions of β'-brass (50.5 wt. % Zn) with reduced volume of the unit cell. The straight lines are least-squares fits to the data points. When pressure is applied, two absorption lines are observed which shift with a slightly different rate.

ready mentioned, according to the Hume-Rothery rules and to a simple band-structure model the number of outer electrons (conduction electrons) per atom is higher in β'- than in α-brass.

The splitting into two absorption lines is not due to the quadrupole interaction, which would give rise to a three-line pattern[32] but seems to originate from two different Cu-Zn surroundings. We emphasize two models.

(1) At high pressures, a new crystallographic phase develops with two inequivalent Zn sites. Such a model, however, is not supported by our compressibility data, which show no hints of a phase transformation up to $\sim$10 GPa. Unfortunately, the x-ray measurements could only be performed at room temperature. To rule out a phase change completely, compressibility data have to be taken at 4.2 K, where all the Mössbauer experiments were carried out. Such measurements are in progress.

(2) At high pressures and low temperatures, a phase change occurs due to a martensitic transition. Such transitions in β'-brass were found earlier,[33,34] however, at relatively low Zn concentrations (between 38 and 43 wt. %). In Ref. 33 a transition $\beta' \rightarrow \beta' + \beta''$ was observed at low temperatures (low-temperature martensite), whereas in Ref. 34 a martensitic transition $\beta' \rightarrow \beta' + \alpha_1$ is described which is caused by mechanical deformation. The determination of the structures β'' and α_1 appears to be difficult. Whereas β'' was attributed to a slightly distorted β' phase, α_1 was claimed to crystallize with fcc structure, similar to the α phase but tetragonally distorted. Our Mössbauer data indicate that distortions would have to be small, since we do not see any hints of a quadrupole interaction.

It is possible that under high pressures these types of martensitic transformations occur at higher Zn concentrations. This suggestion is supported by critical resolved stress measurements as a function of alloy composition.[35,36] Also, the observation that the effective Debye temperature of the martensitic phase is higher than that of the β phase[37] is in agreement with the more negative line position of D_1 (see Fig. 9) caused by an increased second-order Doppler shift. To clarify these questions, x-ray diffraction measurements have to be performed at high pressures and low temperatures.

3. (α,β') *mixed phase containing 44.1 wt. % Zn*

The Mössbauer spectra (see Fig. 4) display a superposition of absorption lines due to the α and β' phases, whereas the β' line clearly dominates. This is expected, since the Zn concentration is rather close to the boundary of the β' phase (see phase diagram of Fig. 1). The relative intensities of the absorption lines do not change with pressure; in fact, the volume dependence of all Mössbauer parameters shows the coexistence of α and β' phases with no indication of a phase transformation from β' to α phase or vice versa.

V. CONCLUSIONS

High-pressure Mössbauer experiments up to $\sim$6 GPa on the α and β' phases of the Cu-Zn alloy system were performed at low temperatures. With reduced volume of the unit cell, no phase transformations from the β' to the α phase (or vice versa) were found. The short-range order in α-brass leading to four different Cu-Zn configurations remains unaffected. Most startling is the observation that one Cu-Zn configuration in the α phase exhibits a center shift of its absorption line which nearly coincides with that one of the β' phase. Surprisingly, the latter shows two absorption lines at higher pressures, which may be due to a martensitic transition. To clarify these questions, theoretical cluster calculations are of great importance. At present, even the occurrence of short-range order in the α phase is not understood from a microscopic point of view. Since the Cu and Zn atoms are relatively light and only cubic structures are involved, reliable calculations might be possible on supercomputers presently available.

ACKNOWLEDGMENTS

We would like to thank the Kernforschungszentrum Karlsruhe, especially Dr. H. Schweickert, K. Assmus, and W. Maier, for numerous and careful source irradiations at the cyclotron. We gratefully acknowledge most valuable discussions with Professor Dr. U. Gonser, Werkstoffwissenschaften, Universität des Saarlandes, Saarbrücken. This work has been funded by the German Federal Minister for Research and Technology [Bundesminister für Forschung und Technologie (BMFT)] under Contract No. 03-KA1TUM-4 and by the Kernforschungszentrum Karlsruhe.

[1]V. Heine and D. Weaire, in *Solid State Physics,* edited by H. Ehrenreich, F. Seitz, and D. Turnbull (Academic, New York, 1970), Vol. 24, p. 249.
[2]J. Hafner and V. Heine, J. Phys. F **13**, 2479 (1983).
[3]A. Bansil, H. Ehrenreich, L. Schwartz, and R. E. Watson, Phys. Rev. B **9**, 445 (1974).
[4]R. Zeller and P. H. Dederichs, Phys. Rev. Lett. **42**, 1713 (1979).
[5]R. Prasad, S. C. Papadopoulos, and A. Bansil, Phys. Rev. B **23**, 2607 (1981).
[6]R. Prasad and A. Bansil, Phys. Rev. Lett. **48**, 113 (1982).
[7]G. M. Stocks, M. Boring, D. M. Nicholson, F. J. Pinski, D. D. Johnson, J. S. Faulkner, and B. L. Gyorffy, in *Noble Metal Alloys,* edited by T. B. Massalski, L. H. Bennett, W. B. Pearson, and Y. A. Chang (The Metallurgical Society of AIME, New York, 1985), p. 27.
[8]M. Hansen and K. Anderko, *Constitution of Binary Alloys* (McGraw-Hill, New York, 1958), p. 650; R. P. Elliott, *Constitution of Binary Alloys,* 1st Suppl. (McGraw-Hill, New York, 1965), p. 390; C. J. Smithells, *Metals Reference Book,* 4th ed. (Butterworths, London, 1967), Vol. II.
[9]W. Hume-Rothery, J. Instrum. Methods **35**, 307 (1926).
[10]W. Potzel, U. Närger, Th. Obenhuber, J. Zänkert, W. Adlassnig, and G. M. Kalvius, Phys. Lett. **98A**, 295 (1983).
[11]W. Potzel, W. Adlassnig, U. Närger, Th. Obenhuber, K. Riski, and G. M. Kalvius, Phys. Rev. B **30**, 4980 (1984).
[12]W. Potzel, W. Adlassnig, J. Moser, C. Schäfer, M. Steiner, and G. M. Kalvius, Phys. Rev. B **39**, 8236 (1989).
[13]I. Dézsi, A. Balogh, J. Balogh, Zs. Kajcsos, D. L. Nagy, and E. Zsoldos, J. Phys. F **9**, 999 (1979).
[14]Th. Obenhuber, W. Adlassnig, J. Zänkert, U. Närger, W. Potzel, and G. M. Kalvius, Hyperfine Interact. **33**, 69 (1987).
[15]Th. Obenhuber, W. Adlassnig, U. Närger, J. Zänkert, W. Potzel, and G. M. Kalvius, Europhys. Lett. **3**, 989 (1987).
[16]Th. Obenhuber, W. Adlassnig, J. Zänkert, U. Närger, W. Potzel, and G. M. Kalvius, Hyperfine Interact. **28**, 1033 (1986).
[17]W. Adlassnig, W. Potzel, J. Moser, C. Schäfer, M. Steiner, and G. M. Kalvius, Nucl. Instrum. Methods A **277**, 485 (1989).
[18]J. Zänkert, U. Potzel, J. Moser, W. Potzel, Th. Obenhuber, M. Wunsch, G. M. Kalvius, J. Gal, and U. Benedict, High Temp.–High Pressures **16**, 533 (1984).
[19]J. Moser, J. Gal, W. Potzel, G. Wortmann, G. M. Kalvius, B. D. Dunlap, D. J. Lam, and J. C. Spirlet, Physica B+C **102B**, 199 (1980).
[20]A. Eichler and J. Wittig, Z. Angew. Phys. **25**, 319 (1968).
[21]W. Potzel, A. Forster, and G. M. Kalvius, Phys. Lett. **67A**, 421 (1978); J. Phys. (Paris) Colloq. **40**, C2-29 (1979).
[22]U. Närger, Diploma thesis, Technische Universität München, Munich, West Germany, 1983.
[23]W. Potzel, Th. Obenhuber, A. Forster, and G. M. Kalvius, Hyperfine Interact. **12**, 135 (1982).
[24]Th. Obenhuber, A. Forster, W. Potzel, and G. M. Kalvius, Nucl. Instrum. Methods **214**, 361 (1983).
[25]G. J. Perlow, W. Potzel, R. M. Kash, and H. de Waard, J. Phys. (Paris) Colloq. **35**, C6-197 (1974).
[26]W. Potzel and N. Halder, Nucl. Instrum. Methods **226**, 418 (1984).
[27]A. Forster, W. Potzel, and G. M. Kalvius, Z. Phys. B **37**, 209 (1980).
[28]P. Bolsaitis and I. L. Spain, in *High Pressure Technology,* edited by I. L. Spain and L. Paauwe (Dekker, New York, 1977), Vol. 1, p. 477.
[29]E. Hornbogen, Z. Metallkd. **78**, 689 (1987).
[30]G. K. Wertheim, M. Campagna, and S. Hüfner, Phys. Condens. Matter **18**, 133 (1974).
[31]W. Adlassnig, Ph.D. thesis, Technische Universität München, Munich, West Germany, 1988.
[32]C. Schäfer, W. Potzel, W. Adlassnig, P. Pöttig, E. Ikonen, and G. M. Kalvius, Phys. Rev. B **37**, 7247 (1988).
[33]G. Bassi and B. Ström, Z. Metallkd. **47**, 16 (1956).
[34]E. Hornbogen, A. Seegmüller, and G. Wassermann, Z. Metallkd. **48**, 379 (1957).
[35]R. Romero and M. Ahlers, J. Phys. F **18**, 563 (1988).
[36]T. Girardeau, J. Mimault, C. Mai, and A. Fontaine, J. Phys. F **18**, 575 (1988).
[37]M. Ahlers, Prog. Mater. Sci. **30**, 135 (1986).